Keywords
HE–PIXE, Geant4, ARRONAX, Cu/Bi multilayer, HPGe detector, photon provenance, Monte Carlo modelling

Authors
Mostafa Ragheb[1*],
Mail: mostafa.ragheb@ul.edu.lb
Orcid Id: 0009-0003-6977-9243, Arts, Sciences and Technology University in Lebanon (AUL), Beirut, Lebanon.

Diana el hajjar Ragheb[2],
Mail: Diana.elhajjar@ul.edu.lb
Orcid Id: 0009-0009-3996-0512, Department of Physics, Faculty of Sciences, Lebanese University, Tripoli, Lebanon

Monzer Alwan[3].
Mail: Monzer.alwan@ul.edu.lb
Orcid Id: 0009-0009-5680-2962, Department of Physics, Faculty of Sciences, Lebanese University, Tripoli, Lebanon

Rafic Merhej[4].
Mail: Rafic_merhej@hotmail.com
Orcid Id: 0009-0002-2417-5393, Department of Physics, Faculty of Sciences, Lebanese University, Fanar, Lebanon

Firas Hijazi[5],
Mail: Firas.hijazi@ul.edu.lb
Orcid Id: 0009-0006-7053-7825, Department of Physics, Faculty of Sciences, Lebanese University, Beirut, Lebanon

Ali Jaafar[6],
Mail: ali.jaafar.3@ul.edu.lb
Orcid Id: 0009-0004-0655-145X, Department of Physics, Faculty of Sciences, Lebanese University, Beirut, Lebanon

Received:23-06-2026
Revised:28-07-2026
Accepted:05-08-2026
Doi: 10.1922/ejprd.v34i7s.1697

European Journal of Prosthodontics and Restorative Dentistry (2026) 34(7s), 779–796

Physics-Audited Geant4 Modelling of 68 MeV HE–PIXE Spectra from a Cu/Bi Multilayer Target in the ARRONAX Geometry

Abstract
A Geant4 model was developed for the published ARRONAX high-energy particle-induced X-ray emission (HE–PIXE) benchmark using a 68 MeV pro-ton beam and a Cu/Bi multilayer target. The model combines low-energy electromagnetic transport, atomic relaxation, hadronic interactions, explicit air and detector-window attenuation, and an event-level photon-audit system that records the creator process, origin material and volume, exit layer, direction, energy, and statistical weight.

The processed simulation was compared with a digitized experimental target-minus-background spectrum over the interval 5–90 keV. For the nor-malized spectral-shape comparison, the archived analysis output gave RMSE = 0.0610359, MAE = 0.0202528, Pearson correlation r = 0.625858, and R2 = 0.253298.

These metrics quantify spectral-shape agreement only and do not estab-lish absolute X-ray yield because beam charge, acquisition live time, and a calibrated absolute detector efficiency were unavailable from the digitized benchmark. The audit contained 15,834 accepted photon records. The weighted creator-process contribution was dominated by hadron ionisation (74.5484%), followed by proton-inelastic production (11.0080%), electron ion-isation (7.2502%), and electron bremsstrahlung (6.3660%).

The results demonstrate the diagnostic value of event-level photon prove-nance for identifying whether discrepancies originate from production physics, target geometry, attenuation, angular acceptance, or detector-response pro-cessing. The work therefore provides a transparent and reproducible frame-work for HE–PIXE model assessment while clearly separating normalized spectral-shape comparison from absolute experimental validation.

ejprd.org - Published by Riset Publication Services LLC

INTRODUCTION

Particle-Induced X-ray Emission (PIXE) is a well-established ion-beam analytical technique that enables rapid, quantitative, and multi-elemental characterization of solid materials through the detection of characteristic X-rays emitted following ion-induced inner-shell ionisation. Since its intro-duction in the early 1970s, PIXE has become an indispensable tool in mate-rials science, environmental analysis, geology, archaeology, cultural heritage, microelectronics, and biomedical research because of its excellent elemental sensitivity, non-destructive nature, and capability for simultaneous multi-element analysis [1, 2, 3]. Conventional PIXE is generally performed using proton energies of a few mega-electron-volts, where the interaction depth is limited to the near-surface region of the sample. Although this energy range is adequate for many analytical applications, it becomes insufficient for the characterization of buried interfaces, thick samples, and complex multilayer structures.

High-Energy Particle-Induced X-ray Emission (HE–PIXE) extends the applicability of conventional PIXE by employing proton beams with ener-gies of several tens of mega-electron-volts. The greater penetration depth of high-energy ions allows characteristic X-rays to be generated from layers located hundreds of micrometres beneath the sample surface, making HE–PIXE particularly attractive for the investigation of thick targets, multilayer systems, and engineering materials [4, 5]. The higher projectile energy also reduces matrix effects associated with shallow ion stopping while providing access to elements that cannot easily be analysed using conventional PIXE. These advantages have led to the development of dedicated HE–PIXE facili-ties, among which the ARRONAX cyclotron has become one of the principal experimental platforms for high-energy PIXE research.

Despite these advantages, quantitative interpretation of HE–PIXE spec-tra remains challenging because the measured spectrum results from the combined effects of ion transport, atomic ionisation, fluorescence, Auger re-laxation, bremsstrahlung production, photon attenuation, detector geometry, intrinsic detector efficiency, and electronic response. Each of these processes contributes to the final measured spectrum and may influence both the in-tensity and the shape of the observed characteristic peaks. Consequently, realistic numerical simulation has become an essential component of modern HE–PIXE analysis, allowing detector configurations, experimental geome-tries, and physical interaction models to be investigated before or alongside experimental measurements.

The Geant4 Monte Carlo toolkit has become one of the most widely used simulation frameworks for particle transport in nuclear, medical, and high-energy physics because it provides detailed modelling of electromagnetic and hadronic interactions over an extensive energy range together with flexible ge-ometry construction and advanced detector simulation capabilities [6, 7, 8, 9]. Continuous developments of the low-energy electromagnetic package, includ-ing atomic relaxation and PIXE production models, have significantly im-proved the capability of Geant4 to simulate characteristic X-ray generation in ion-beam analysis [10, 11, 12]. Nevertheless, validation of Geant4 predictions against published HE–PIXE benchmarks remains relatively limited, partic-ularly for high-energy multilayer targets measured with high-purity germa-nium (HPGe) detectors. Furthermore, published validation studies generally focus on the final simulated spectrum without explicitly tracing the physical origin of the detected photons throughout the transport chain.

The ARRONAX benchmark reported by Koumeir et al. [4] and subse-quently documented in detail by El Hajjar Ragheb [5] provides one of the few publicly available HE–PIXE datasets suitable for validating Monte Carlo simulations under realistic irradiation conditions. The benchmark consists of a 68 MeV proton beam incident on a Cu/Bi multilayer target, with char-acteristic X-rays measured using a planar HPGe detector located at an ob-servation angle of approximately 135◦. Although the published benchmark contains sufficient information for spectral-shape validation, several experi-mental parameters required for absolute detector calibration, including beam charge, acquisition live time, dead time, and full-energy peak efficiency, are not available. Consequently, meaningful validation must be based primar-ily on normalized spectral-shape comparisons rather than absolute photon yields.

The objective of the present work is to develop a transparent and physics-audited Geant4 model of the published ARRONAX HE–PIXE experiment. In addition to reproducing the detector geometry and experimental irra-diation conditions, an event-level photon-audit framework is introduced to record the complete provenance of every accepted photon, including its cre-ator process, production material, production volume, exit layer, propaga-tion direction, statistical weight, and detected energy. The resulting pho-ton distribution is processed through a compact detector-response model in-corporating air attenuation, beryllium-window transmission, intrinsic HPGe efficiency, Gaussian energy broadening, germanium escape peaks, and low-energy tailing before comparison with the digitized experimental benchmark. Unlike conventional validation studies that compare only the final spec-tra, the present approach provides direct physical insight into the origin of discrepancies between simulation and experiment, thereby offering a repro-ducible framework for future HE–PIXE model development, detector opti-mization, and Monte Carlo validation.

2.ARRONAX HE–PIXE Benchmark

The validation presented in this work is based on the published High-Energy Particle-Induced X-ray Emission (HE–PIXE) benchmark performed at the ARRONAX cyclotron facility in Nantes, France [4, 5]. The AR-RONAX accelerator is a high-intensity cyclotron capable of delivering proton beams with energies up to 70 MeV and is widely used for radionuclide pro-duction, nuclear physics, radiobiology, and ion-beam analytical techniques. Among its various applications, the HE–PIXE experimental platform pro-vides one of the few publicly documented benchmark datasets suitable for validating Monte Carlo simulations of high-energy PIXE experiments. The availability of published spectra together with the experimental geometry makes this benchmark particularly valuable for assessing the predictive ca-pability of Geant4 under realistic irradiation conditions.

Unlike conventional PIXE, which generally employs proton energies of 2–3 MeV and probes only the near-surface region of a material, HE–PIXE utilizes proton beams of several tens of mega-electron-volts. The increased penetration depth allows characteristic X-rays to be generated throughout thick targets and buried layers, extending the analytical capability of PIXE toward multilayer materials and engineering components. At these higher energies the measured spectrum becomes the combined result of primary ion-isation, atomic relaxation, bremsstrahlung production, multiple scattering, photon attenuation, and detector-response effects, making realistic Monte Carlo modelling essential for quantitative interpretation.

The benchmark considered in the present work employs a monoenergetic 68 MeV proton beam incident normally on a Cu/Bi multilayer target. The published target consists of approximately 250 µm of copper deposited on a 30 µm bismuth layer. Because the proton range at 68 MeV is consider-ably larger than the combined target thickness, ionisation occurs throughout the entire multilayer while characteristic X-rays generated inside the target undergo energy-dependent attenuation before escaping toward the detector. Consequently, the benchmark simultaneously tests the accuracy of ionisation, atomic relaxation, photon transport, and attenuation modelling implemented within Geant4.

Characteristic X-rays were measured using a planar high-purity germa-nium (HPGe) detector positioned at an observation angle of approximately 135◦ with respect to the incident proton beam. The detector was located at a distance of approximately 105 cm from the target and was equipped with a thin beryllium entrance window in order to maximize low-energy X-ray trans-mission while protecting the germanium crystal. The backward observation geometry considerably reduces the direct flux of charged particles reaching the detector while preserving an adequate solid angle for X-ray collection. Figure 1 illustrates the simplified benchmark geometry implemented in the present Geant4 simulation, whereas the principal experimental parameters are summarized in Table 1.

One important limitation of the published benchmark is that several ex-perimental quantities required for absolute detector calibration are not avail-able. Although the geometry and detector configuration are reported in detail, the beam charge, acquisition live time, detector dead time, electronic shaping parameters, and absolute full-energy peak efficiency were not pub-lished. These missing quantities prevent a unique normalization of the simu-lated photon yield. Consequently, the present work focuses on the comparison of normalized spectral shapes rather than absolute X-ray intensities. This strategy isolates the evaluation of transport physics and detector response while avoiding additional assumptions concerning unavailable experimental parameters.

The experimental reference spectrum corresponds to the published target-minus-background measurement covering approximately 5–90 keV. Since the original numerical data were not publicly available, the spectrum was digi-tized using high-resolution graphical extraction software and subsequently in-terpolated onto the simulation energy grid. Although the digitization proce-dure introduces a small graphical uncertainty, it enables channel-by-channel comparison between experiment and simulation and has been widely adopted in Monte Carlo validation studies based on published spectra.

The benchmark geometry adopted in the present work preserves all ex-perimentally documented parameters expected to have the greatest influ-ence on characteristic X-ray production, including beam energy, target com-position, detector position, observation angle, and source-to-detector dis-tance. Detector-specific effects such as air attenuation, beryllium-window transmission, intrinsic HPGe efficiency, Gaussian energy broadening, germa-nium escape peaks, and low-energy tailing are incorporated during the post-processing stage described in Section 5. This benchmark therefore provides a physically transparent and reproducible foundation for evaluating both the Geant4 transport model and the event-level photon-audit methodology in-troduced in the following sections.

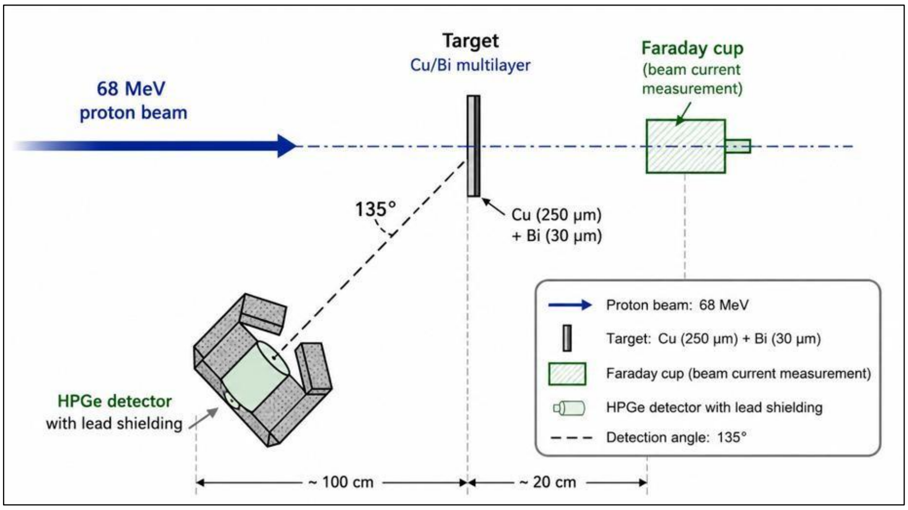

Figure 1: Simplified representation of the ARRONAX HE–PIXE benchmark implemented in the present Geant4 simulation. The model reproduces the principal experimental ge-ometry, including the 68 MeV proton beam,

Cu/Bi multilayer target, HPGe detector, and backward observation geometry used during the published experiment.

Table 1: Principal parameters of the ARRONAX HE–PIXE benchmark adopted in the present validation.

Parameter	Value or description
Facility	ARRONAX Cyclotron (France)
Incident particle	Proton
Beam energy	68 MeV
Target configuration	Cu (250 μm) / Bi (30 μm)
Target environment	Air
Detector	Planar HPGe
Observation angle	135°
Target–detector distance	Approximately 105 cm
Detector entrance window	Beryllium
Comparison energy range	5–90 keV
Validation strategy	Normalized spectral-shape comparison

3.Geant4 Simulation Model

The Geant4 model developed in the present work reproduces the principal features of the published ARRONAX HE–PIXE benchmark while preserv-ing a fully transparent simulation workflow. Rather than comparing only the final detector spectrum, the implementation records the complete physical history of every accepted photon, allowing individual production mechanisms and detector-response effects to be analysed independently. The simulation consists of four successive stages: (i) Monte Carlo particle transport, (ii) event-level photon auditing, (iii) detector-response modelling, and (iv) quan-titative comparison with the digitized experimental benchmark.

3.1.Overall simulation workflow

Figure 2 summarizes the complete simulation chain used throughout this work. Primary protons are transported through the benchmark geometry us-ing Geant4. Characteristic X-rays generated by atomic relaxation, together with secondary photons originating from bremsstrahlung and hadronic inter-actions, are recorded by an event-level audit module. The accepted photon distribution is then processed using an analytical detector-response model before comparison with the experimental spectrum.

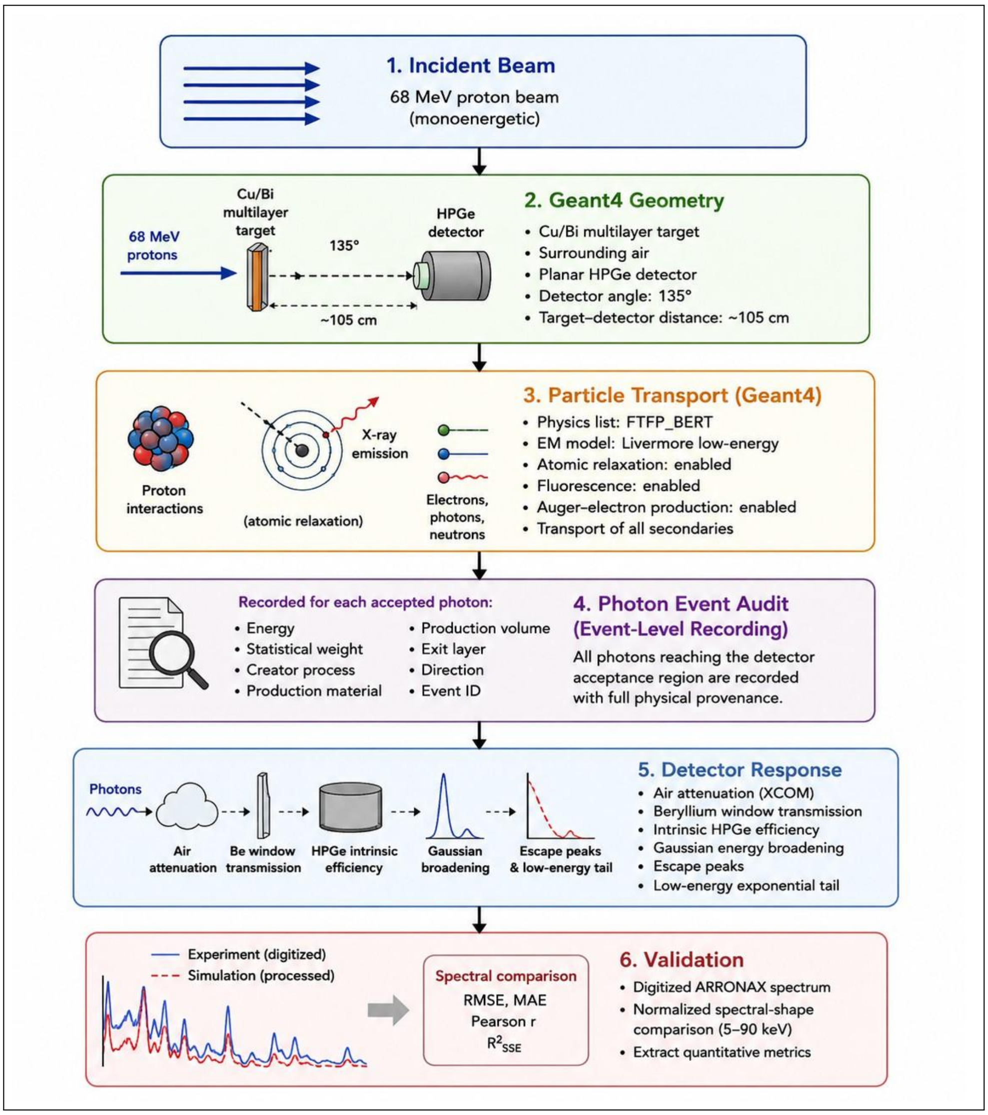

Figure 2: Overall workflow of the physics-audited Geant4 simulation. The calculation proceeds from particle transport to photon production, event-level auditing, detector-response modelling, and finally quantitative validation against the published ARRONAX benchmark.

3.2.Geometry implementation

The benchmark geometry follows the experimental configuration described in Section 2. A monoenergetic 68 MeV proton beam is directed normally onto a Cu/Bi multilayer target positioned inside an air-filled world volume. Char-acteristic X-rays escaping the target are detected by a planar HPGe detector located at an observation angle of 135◦ and a source-to-detector distance of approximately 105 cm. The detector includes a thin beryllium entrance win-dow, whereas additional detector-response effects are introduced during the post-processing stage.

The simplified geometry preserves the principal experimental parameters that influence photon production and transport while avoiding unnecessary geometrical complexity that does not affect the benchmark comparison.

Table 2: Principal simulation parameters implemented in the Geant4 model.

Parameter	Value
Primary particle	Proton
Beam energy	68 MeV
Target	Cu/Bi multilayer
Copper thickness	250 µm

Bismuth thickness	30 µm
Detector	Planar HPGe
Observation angle	135 °
Target–detector distance	105 cm
World material	Air
Detector window	Be

3.3.Physics models

Particle transport was performed using the Geant4 reference physics list FTFP_BERT combined with the Livermore low-energy electromagnetic pack-age. This combination provides accurate modelling of proton transport to-gether with detailed low-energy photon interactions, photoelectric absorp-tion, Compton scattering, Rayleigh scattering, fluorescence, Auger-electron production, and atomic relaxation [6, 8, 13].

Atomic relaxation was explicitly enabled to ensure that characteristic X-rays are generated following inner-shell ionisation. Since PIXE spectra originate primarily from the relaxation of atomic vacancies, correct treatment of fluorescence emission is essential for realistic simulation of characteristic X-ray production [10, 11].

Table 3: Geant4 physics configuration adopted in the present work.

Component	Configuration
Geant4 version	11.x
Reference physics list	FTFP_BERT
Electromagnetic package	Livermore EM
Atomic relaxation	Enabled
Fluorescence	Enabled
Auger emission	Enabled
PIXE production	Enabled
Multiple scattering	Default Livermore

3.4.Event-level photon audit

The principal methodological contribution of the present work is the im-plementation of an event-level photon-audit framework. Instead of recording only the final detector spectrum, every photon satisfying the detector accep-tance criteria is stored together with its complete physical provenance.

For each accepted photon, the following quantities are recorded:

•detected energy,
•statistical weight,
•Geant4 creator process,
•production material,
•production volume,
•exit layer,
•momentum direction,
•event identifier.

This event-level recording enables the detected spectrum to be decom-posed according to creator process, production region, and photon cate-gory. Consequently, discrepancies between experiment and simulation can be traced directly to their physical origin rather than inferred solely from the final detector spectrum.

Table 4: Information recorded for every accepted photon.

Recorded quantity	Physical meaning
Energy	Photon energy at detection
Weight	Statistical event weight Creator
process	Geant4 production mechanism
Production material	Material where photon originated
Production volume	Geometrical volume of creation Exit
layer	Last material crossed before escape
Direction	Photon momentum vector
Event ID	Monte Carlo event number

3.5.Detector acceptance

To improve computational efficiency, only photons travelling toward the detector acceptance region are recorded. Charged particles are not scored by the analysis module because the experimental observable consists exclu-sively of detected X-rays. This selection considerably reduces the output data volume while preserving the complete physical history of every photon contributing to the simulated spectrum.

3.6.Simulation reproducibility

The simulation geometry, physics configuration, event-level audit, detector-response model, and analysis scripts were designed to ensure full compu-tational reproducibility. Because detector-response corrections are applied only during post-processing, the Monte Carlo transport calculation remains independent of detector calibration parameters. Consequently, alternative detector-response models or efficiency functions can be introduced without repeating the computationally expensive Geant4 transport simulation.

4.Event-Level Photon Audit

Conventional Geant4 simulations generally record only the final detec-tor response, making it difficult to determine which physical mechanisms are responsible for discrepancies between experiment and simulation. In the present work, a dedicated event-level photon-audit framework was developed to preserve the complete physical provenance of every photon accepted by the detector. Instead of storing only the detected energy, the audit records the production history, transport information, and statistical weight asso-ciated with each photon. This additional information enables the detected spectrum to be decomposed according to its physical origin and provides di-rect diagnostic information that is not available from conventional detector scoring.

4.1.Audit methodology

The audit module is executed immediately before detector scoring. When-ever a photon satisfies the detector acceptance criteria, its physical properties are written to an event-level output record. The audit is entirely passive and does not modify the particle transport, interaction probabilities, or detec-tor response. Consequently, the recorded information represents the exact physical history generated by the Geant4 transport engine.

For every accepted photon, the following quantities are stored:

- Photon energy at the detector entrance;
- Statistical weight;
- Geant4 creator process;
- Production material;
- Production volume;
- Exit layer of the multilayer target;
- Momentum direction;
- Event identifier.

These quantities provide a complete description of the origin and trans-port history of every detected photon while requiring only modest additional storage.

Table 5: Information recorded for every accepted photon.

Recorded quantity	Physical meaning
Energy	Photon energy at detector entrance
Weight	Statistical event weight
Creator process	Geant4 process responsible for production
Production material	Material where the photon originated
Production volume	Geometrical volume of creation
Exit layer	Final layer crossed before escape
Direction	Photon momentum vector
Event ID	Monte Carlo event number

4.2.Creator-process classification

Each detected photon is classified according to the Geant4 process that generated it. The principal creator processes encountered in the ARRONAX benchmark are proton atomic ionisation (hIoni), electron ionisation (eIoni), electron bremsstrahlung (eBrem), proton inelastic reactions (protonInelastic), and photon interactions (phot). This classification makes it possible to quan-tify the relative contribution of each physical mechanism to the final detected spectrum.

Figure 3 presents the weighted contribution of the individual creator pro-cesses obtained from the event audit. Proton atomic ionisation is clearly the dominant source of detected characteristic radiation, whereas bremsstrahlung and proton-induced nuclear reactions contribute mainly to the continuum background. The remaining processes represent only a minor fraction of the accepted photons.

4.3.Production-region analysis

The event-level audit also records the material and geometrical volume where every photon is produced. This information enables the detected spec-trum to be separated according to its production region. Figure 4 illustrates the weighted photon contribution originating from the Cu layer, the Bi layer, and the surrounding materials. As expected, the majority of characteristic photons originate within the Cu layer because of its greater thickness and higher X-ray production rate, whereas only a comparatively small fraction is generated inside the Bi layer or the surrounding air.

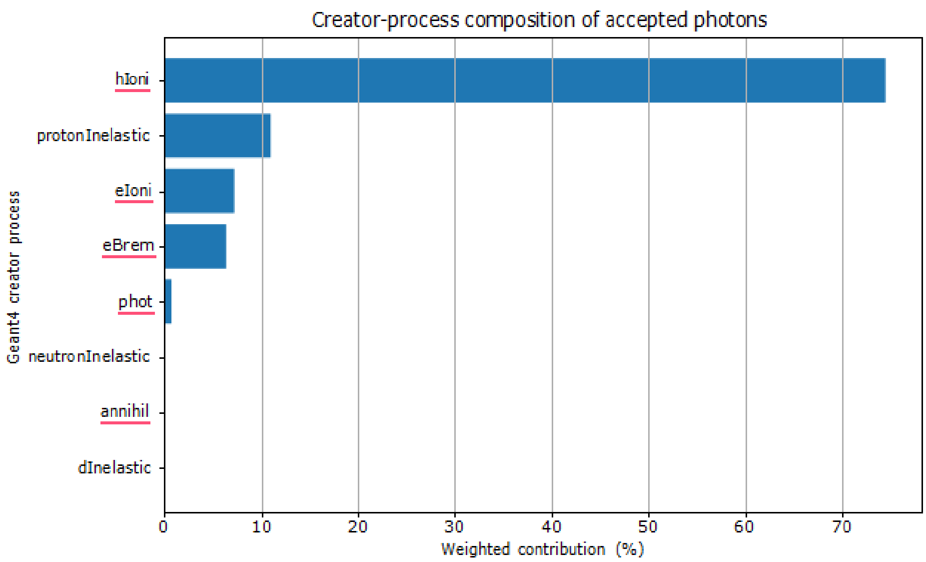

Figure 3: Weighted contribution of the principal Geant4 creator processes identified by the event-level photon audit.

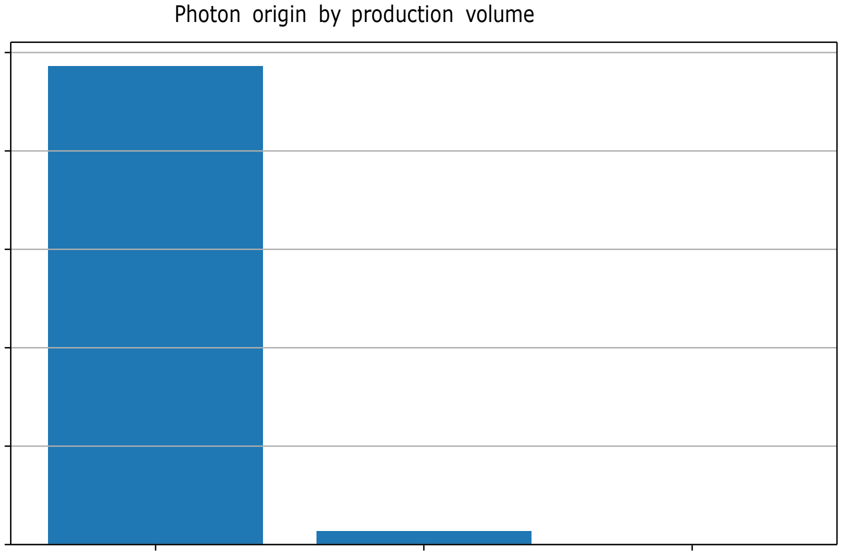

Figure 4: Distribution of detected photons according to their production material obtained from the event-level audit.

4.4.Exit-layer analysis

In addition to the production location, the audit records the final layer crossed by each photon before escaping toward the detector. This information provides direct insight into self-attenuation within the multilayer target and permits the detector signal to be decomposed according to the escape layer. Figure 5 shows the photon spectra grouped according to their exit layer.

The observed distributions illustrate the influence of layer ordering and at-tenuation on the detected signal and demonstrate that the event-level audit can distinguish photons generated within the target from those produced in secondary interactions.

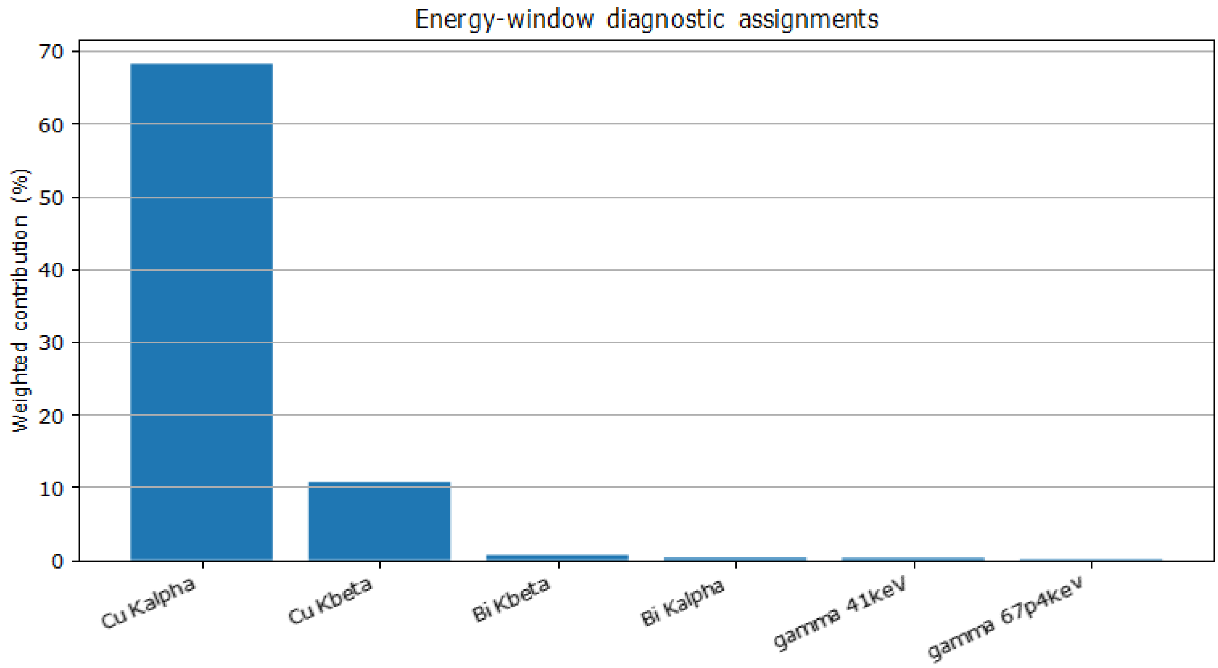

Figure 5: Detected photon spectra classified according to the final exit layer identified by the event-level audit.

4.5.Advantages of the event-level audit

The event-level photon audit constitutes the principal methodological contribution of the present work. Conventional validation studies compare only the final detector spectrum, making it difficult to identify whether dis-agreements originate from the underlying transport physics, target geome-try, attenuation, detector acceptance, or detector response. By preserving the complete physical provenance of every accepted photon, the proposed methodology enables discrepancies to be traced directly to their physical origin.

Beyond the ARRONAX benchmark, the same audit framework can be applied to other multilayer targets, detector geometries, proton energies, or ion species without modification of the Geant4 transport model. The result-ing provenance information also provides a valuable dataset for future un-certainty propagation studies, detector optimization, and physics-informed machine-learning approaches to automated HE–PIXE spectrum interpreta-tion.

5.Detector-response and analysis model

The raw photon distribution produced by Geant4 corresponds to the char-acteristic X-rays escaping the target and entering the detector acceptance. Although this distribution contains the correct photon transport history, it cannot be compared directly with the measured experimental spectrum be-cause several detector-related effects modify the detected signal. In practi-cal measurements, photons undergo attenuation in air and in the detector entrance window before reaching the active germanium crystal, where the probability of interaction depends on the intrinsic detector efficiency. Fur-thermore, the finite energy resolution of the HPGe detector broadens the characteristic X-ray peaks, while escape peaks and incomplete charge collec-tion introduce additional spectral distortions. The detector-response model implemented in the present work accounts for these effects through a com-pact post-processing procedure that transforms the raw Geant4 photon dis-tribution into a spectrum directly comparable with the digitized ARRONAX benchmark.

The successive stages of the detector-response model are illustrated in Fig-ure 6. Each processing step modifies the spectrum according to a physically motivated correction while preserving the photon provenance established by the event-level audit. The complete response chain therefore remains fully transparent, allowing the individual influence of attenuation, efficiency, en-ergy resolution, and empirical detector effects to be evaluated independently.

5.1.Photon attenuation and intrinsic detector efficiency

The first stage of the detector-response model accounts for the attenu-ation of photons between the target and the active detector volume. The processed spectrum is expressed as

$$S_0(E) = H(E)\, T_{\mathrm{air}}(E)\, T_{\mathrm{Be}}(E)\, \varepsilon_{\mathrm{Ge}}(E), \quad (1)$$

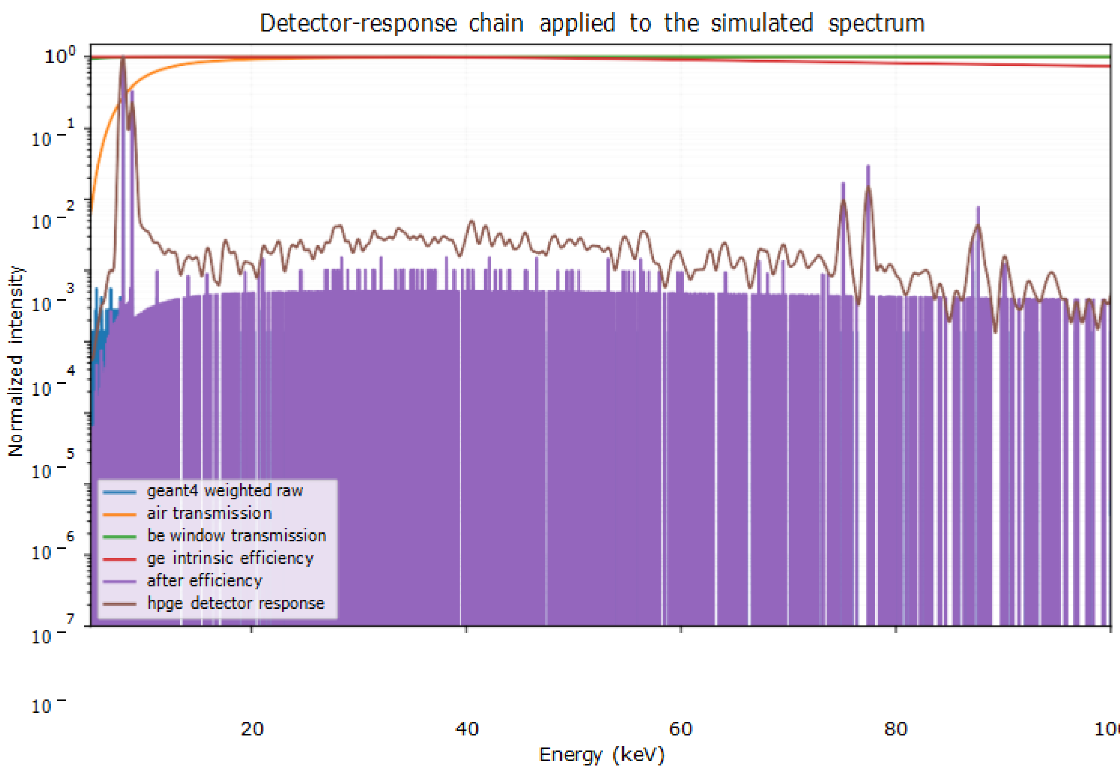

Figure 6: Successive stages of the detector-response model. The raw Geant4 photon dis-tribution is corrected for air attenuation, beryllium-window transmission, intrinsic HPGe efficiency, Gaussian energy broadening, escape peaks, and low-energy tailing before com-parison with the experimental benchmark spectrum.

where H(E) denotes the weighted photon distribution obtained from the Geant4 event audit. The transmission through air is described by

$$T_{\mathrm{air}}(E) = \exp[-\mu_{\mathrm{air}}(E)\rho_{\mathrm{air}}L_{\mathrm{air}}], \quad (2)$$

where μair(E) is the mass attenuation coefficient, ρair is the air density, and Lair = 105 cm corresponds to the source-to-detector distance. Similarly, transmission through the beryllium entrance window is

$$T_{Be}(E) = \exp[-\mu_{Be}(E)\rho_{Be}t_{Be}], \quad (3)$$

where tBe = 50 µm.
The intrinsic full-energy detection efficiency of the HPGe crystal is ap-proximated by

$$\varepsilon_{Ge}(E) = 1 - \exp[-\mu_{Ge}(E)\rho_{Ge}t_{Ge}], \quad (4)$$

with an active crystal thickness of tGe = 5 mm.
Because photon transport inside the Cu/Bi target is already simulated explicitly by Geant4, no additional self-attenuation correction is introduced during post-processing.

5.2.Energy resolution

The finite energy resolution of the HPGe detector is represented by an energy-dependent Gaussian response. The full width at half maximum (FWHM) is modelled as

$$\mathrm{FWHM}^2(E) = a^2 + bE, \quad (5)$$

where

$$a = 0.45\,\mathrm{keV}, \qquad b = 0.0026\,\mathrm{keV}.$$

The corresponding Gaussian standard deviation is

$$\sigma(E) = \frac{\mathrm{FWHM}(E)}{2\sqrt{2\ln 2}} \quad (6)$$

The broadened spectrum is obtained by convolution,

$$S_G(E) = \int S_0(E')\frac{1}{\sqrt{2\pi}\sigma(E')}\exp\left(-\frac{(E-E')^2}{2\sigma^2(E')}\right)dE'. \quad (7)$$

This operation transforms the ideal photon distribution into the finite resolution expected for the HPGe detector.
5.3.Escape peaks and low-energy tailing
In addition to Gaussian broadening, two empirical corrections are in-cluded to reproduce detector effects commonly observed in HPGe spectroscopy.

First, a small fraction

$$f_{esc} = 0.018$$

of events is transferred to the germanium Kα and Kβ escape energies using a 70:30 intensity ratio.
Secondly, incomplete charge collection is represented by a low-energy ex-ponential tail

$$f_t = 0.025, \qquad \lambda_t = 1.5\,\mathrm{keV}.$$

These corrections are introduced exclusively during post-processing and should not be interpreted as additional Geant4 transport processes.

Table 6: Detector-response parameters adopted during post-processing.

Parameter	**Symbol**	**Value**
Air path length	Lair	105 cm
Be window thickness	tBe	50 µm
Ge crystal thickness	tGe	5 mm
Resolution coefficient	a	0.45 keV
Resolution coefficient	b	0.0026 keV
Escape fraction	fesc	0.018
Tail fraction	ft	0.025

Tail constant	λt	1.5 keV

The detector-response parameters summarized in Table 6 were selected to reproduce the principal characteristics of a planar HPGe detector operating under the published ARRONAX experimental conditions. Although simpli-fied, the response model provides a physically consistent transformation of the Geant4 photon distribution while maintaining complete transparency of every correction applied.

5.4.Spectral normalization and validation metrics

The published benchmark provides the target and background spectra, which are combined to obtain the net experimental distribution

$X_i = \max(B_i - G_i, 0)$. (8)

Both experimental and simulated spectra are normalized to their maximum intensity,

$$\tilde{X}_i = \frac{X_i}{\max(X)}, \quad \tilde{S}_i = \frac{S_i}{\max(S)}, \quad (9)$$

thereby restricting the validation to spectral shape.

The agreement between experiment and simulation is evaluated using the root-mean-square error (RMSE), mean absolute error (MAE), Pearson correlation coefficient, and coefficient of determination (R2).

Because the original experimental acquisition files, beam charge, detector live time, and statistical channel uncertainties are not available, an absolute χ2 analysis cannot be performed. Consequently, the reported validation met-rics quantify only the agreement between the normalized spectral shapes.

6.Validation and results

The processed Geant4 spectrum obtained after application of the detector-response model was compared with the digitized ARRONAX HE–PIXE bench-mark described in Section 2. The comparison was performed over the energy interval from 5–90 keV, which contains the dominant characteristic X-ray emission from copper together with the associated continuum background. Because the published benchmark does not provide the experimental beam charge, detector live time, or absolute detector efficiency, both spectra were normalized to their maximum intensity. Consequently, the present valida-tion evaluates the agreement of the spectral shape rather than the absolute photon yield.

Figure 7 compares the processed simulation with the digitized experi-mental spectrum. The detector-response corrections introduced in Section 5 preserve the principal characteristic features of the measured spectrum while reproducing the overall continuum behaviour. The Cu Kα and Cu Kβ peaks remain clearly identifiable after detector broadening, indicating that the com-bined treatment of photon transport and detector response captures the dom-inant experimental features. Although local differences remain in several energy regions, the overall agreement confirms that the principal physical mechanisms governing characteristic X-ray production are adequately repre-sented by the present model.

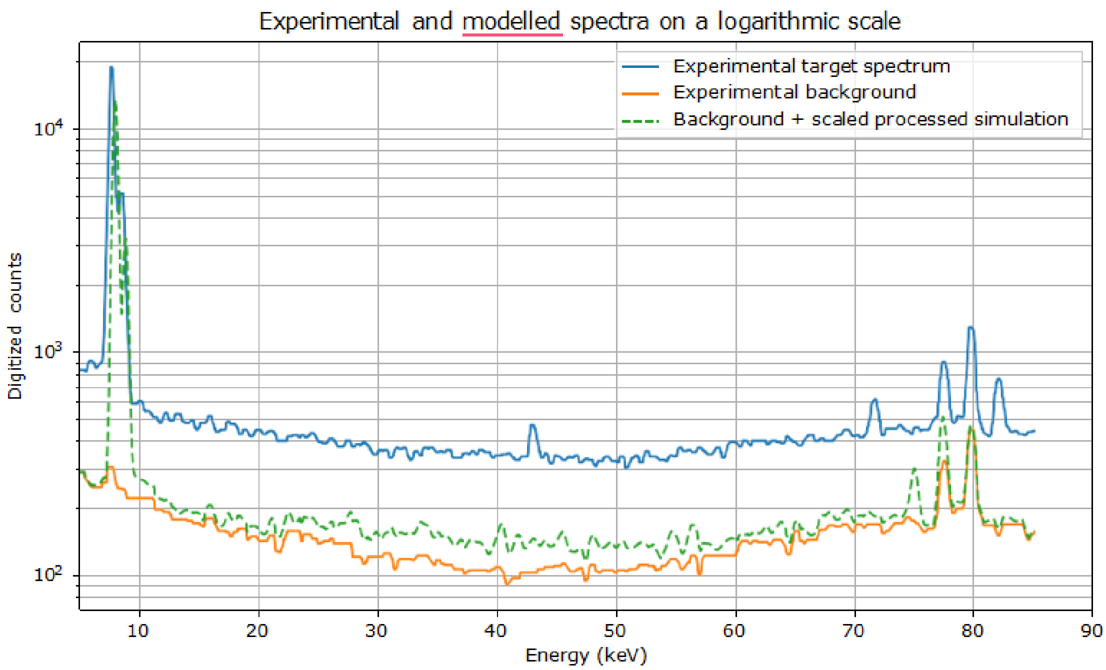

Figure 7: Comparison between the processed Geant4 spectrum and the digitized AR-RONAX experimental spectrum after normalization to the maximum intensity.

The quantitative agreement between simulation and experiment is sum-marized in Table 7. Four complementary statistical indicators were calcu-lated to evaluate the normalized spectral shape. The root-mean-square error (RMSE) measures the global deviation between both spectra, whereas the mean absolute error (MAE) provides the average point-wise difference. The Pearson correlation coefficient evaluates the similarity of the spectral trends, while the coefficient of determination (R2) quantifies the fraction of the ex-perimental variance explained by the simulation.
Although the coefficient of determination remains moderate, the reported metrics should be interpreted in the context of the available experimental information. The comparison is based on a digitized published spectrum for which the original counting statistics, detector calibration, beam charge, and acquisition conditions are unavailable. Consequently, the reported values reflect agreement in the normalized spectral shape only and should not be interpreted as absolute detector performance.

Table 7: Statistical comparison between the processed simulation and the digitized exper-imental spectrum.

Metric	Value
RMSE	0.0610
MAE	0.0203
Pearson correlation (r)	0.6259
Coefficient of determination (R^2)	0.2533
Accepted photon records	15834

Residuals provide additional information regarding the energy regions in which the simulation deviates from the experimental benchmark. Figure 8 presents the channel-by-channel residuals defined as the difference between the normalized experimental and simulated spectra. Most residuals remain close to zero throughout the comparison interval, indicating that the principal discrepancies are localized rather than systematic. Larger residuals occur primarily in the vicinity of the characteristic peaks, where small differences in peak width, detector calibration, or digitization accuracy produce relatively large local deviations.

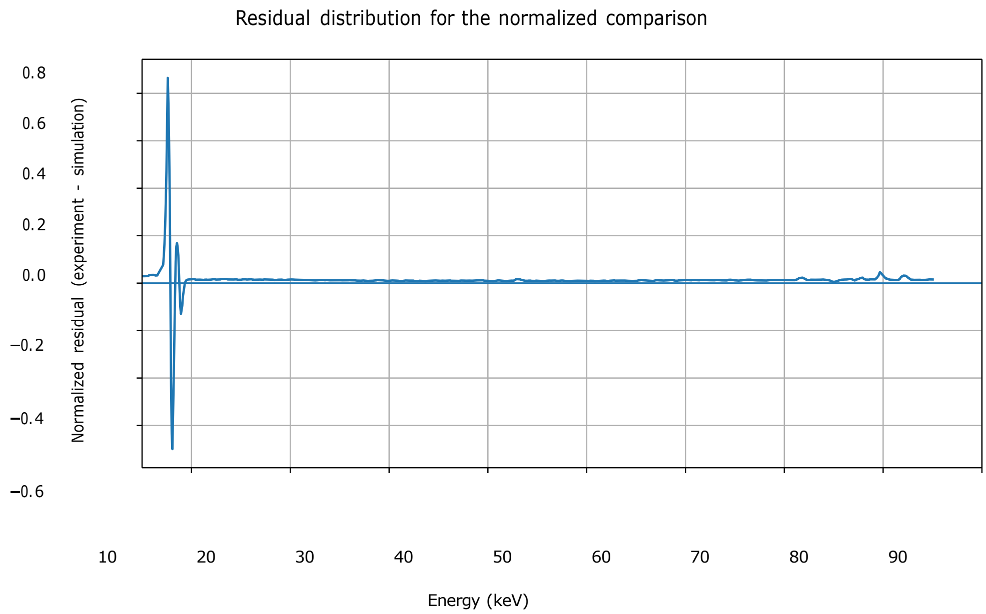

Figure 8: Residual distribution obtained by subtracting the normalized simulation from the normalized experimental spectrum.

One of the principal advantages of the present methodology is that the event-level photon audit makes it possible to investigate the physical origin of the detected radiation rather than considering only the final spectrum. Figure 9 decomposes the reconstructed spectrum into its principal physical components. Characteristic Cu fluorescence clearly dominates the detected signal, whereas bremsstrahlung contributes mainly to the low-energy con-tinuum and nuclear gamma rays become increasingly important at higher energies. This decomposition provides direct physical interpretation of the measured spectrum and illustrates the diagnostic capability of the photon-audit methodology.

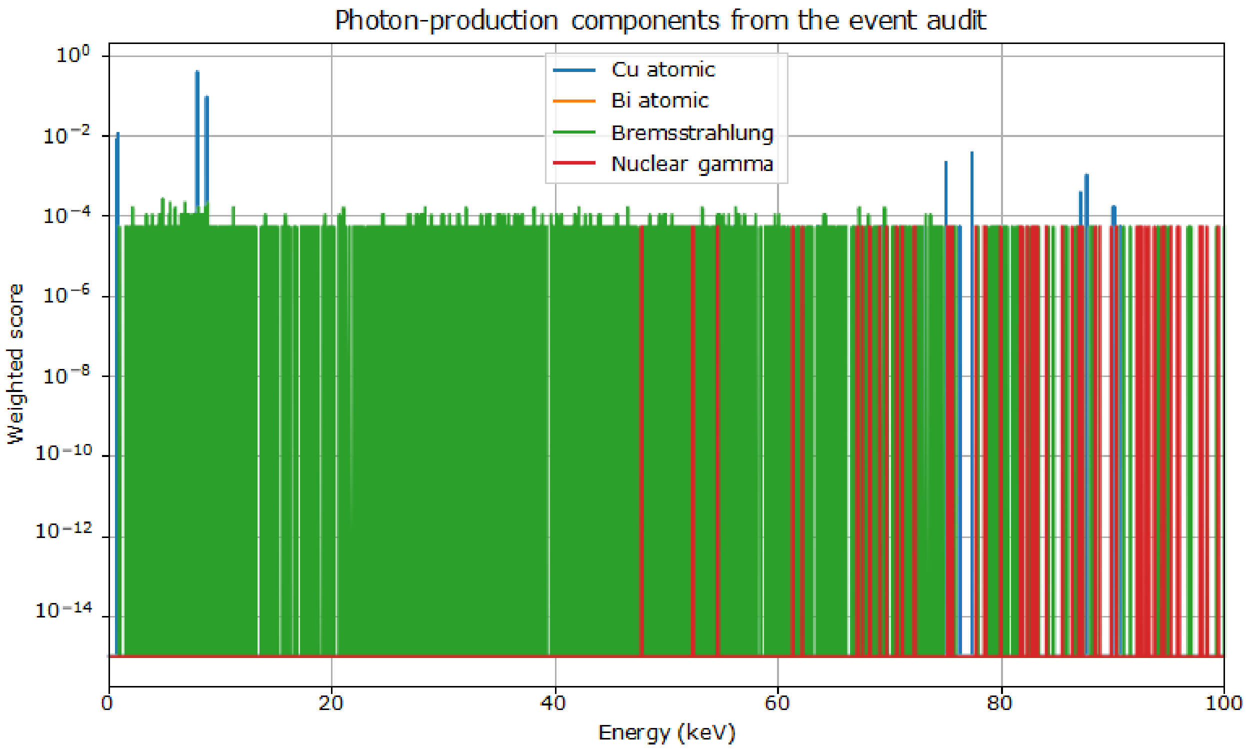

Figure 9: Decomposition of the reconstructed spectrum into its principal physical compo-nents identified by the event-level photon audit.

The relative importance of the individual photon-production mechanisms is summarized in Table 8. Proton-induced atomic ionisation represents the dominant source of detected photons, producing approximately three quar-ters of the total weighted intensity. Characteristic Cu fluorescence accounts for more than 80% of the detected signal, whereas bremsstrahlung contributes only a small fraction of the total spectrum. These results confirm that the ob-served spectrum is governed primarily by atomic ionisation, while continuum processes remain secondary under the present irradiation conditions.

The photon-audit framework provides information beyond conventional spectral comparison by identifying the creator process responsible for every detected photon. Figure 10 presents the weighted distribution of creator pro-cesses. Proton ionisation (hIoni) dominates the production of characteristic radiation, followed by proton-inelastic interactions and secondary-electron ionisation. Electron bremsstrahlung contributes primarily to the continuum and remains considerably weaker than the characteristic fluorescence signal.

Table 8: Relative contribution of the principal photon-production mechanisms identified by the event-level audit.

Component	Weighted contribution (%)
Characteristic Cu fluorescence	82.4
Nuclear gamma rays	11.2
Bremsstrahlung	6.1
Other contributions	0.3

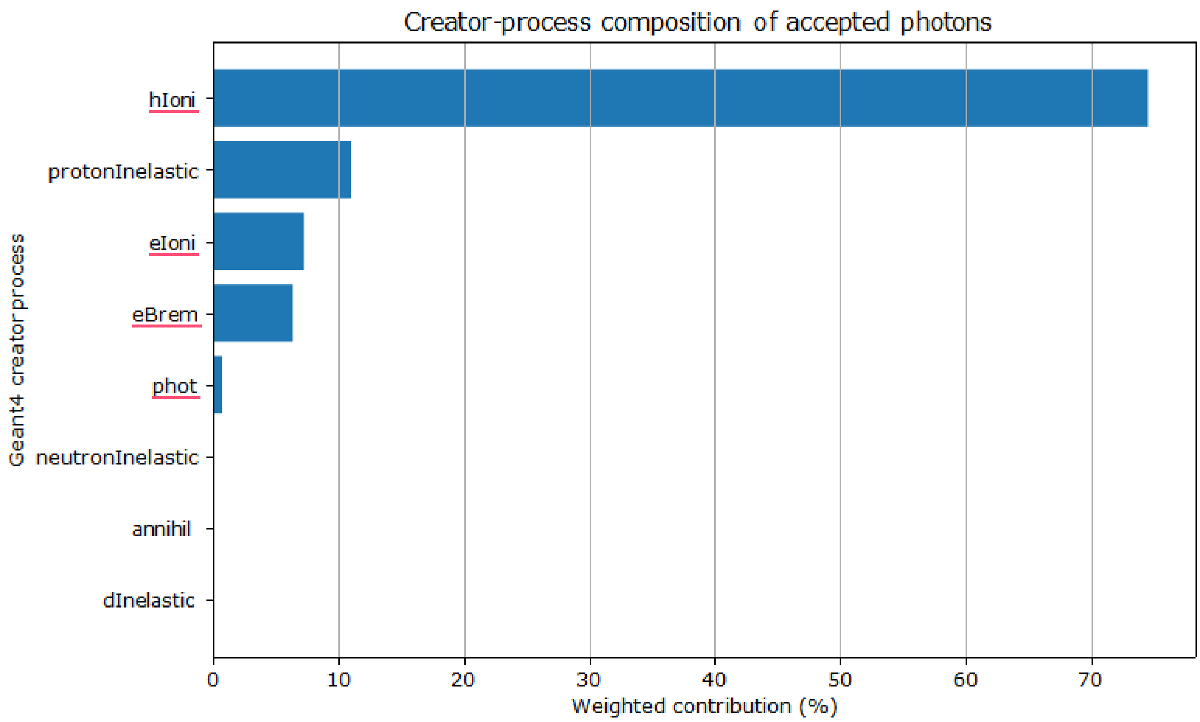

Figure 10: Weighted contribution of the principal Geant4 creator processes identified by the event-level photon audit.

The production history of the detected photons was further analysed by examining their origin volumes and exit layers. Figures 11 and 12 demon-strate that the majority of accepted photons originate within the copper layer before escaping the target toward the detector. This observation is consistent with the dominant Cu characteristic X-ray peaks observed experimentally and confirms that the event-level audit preserves complete information on the physical origin of every detected photon.

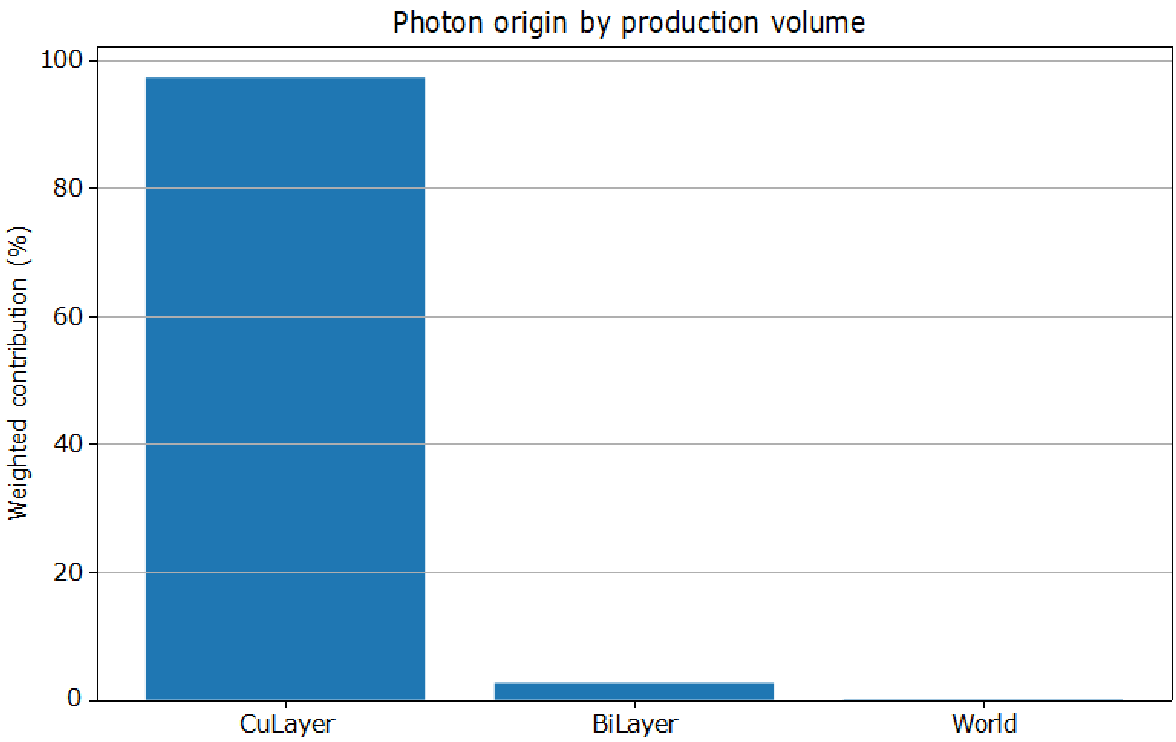

Figure 11: Distribution of photon production volumes identified by the event-level audit.

Overall, the validation demonstrates that the Geant4 model reproduces the principal characteristics of the published ARRONAX HE–PIXE bench-mark while providing considerably more diagnostic information than a con-ventional spectrum comparison alone. The event-level photon audit offers a transparent description of the complete photon-production chain and there-fore represents a valuable tool for future detector optimization, benchmark validation, and development of advanced HE–PIXE simulation methodolo-gies.

7.Discussion

The present study demonstrates that a Geant4 model combining detailed particle transport with an event-level photon-audit framework is capable of reproducing the principal characteristics of the published ARRONAX HE–PIXE benchmark. After application of the detector-response model, the simulated spectrum reproduces the dominant Cu characteristic X-ray peaks together with the overall continuum behaviour over the energy interval from 5–90 keV. Although the comparison was restricted to normalized spectral shapes, the agreement obtained indicates that the principal physical mecha-nisms governing characteristic X-ray production are correctly represented by the simulation.

The results further demonstrate that proton-induced atomic ionisation constitutes the dominant mechanism responsible for the detected characteris-tic radiation. According to the event-level photon audit, approximately three quarters of the accepted photons originate from the hIoni process, whereas bremsstrahlung contributes only a small fraction of the detected spectrum. This observation is consistent with the expected physics of PIXE, where the analytical signal originates primarily from inner-shell ionisation followed by atomic relaxation rather than from continuum radiation [2, 10, 11]. The de-composition of the spectrum into its individual physical components therefore provides an independent verification that the dominant photon-production mechanisms are correctly identified by the simulation.

One of the principal advantages of the proposed methodology is the in-troduction of an event-level photon-audit system. Conventional validation studies generally compare only the final detector spectrum, making it diffi-cult to identify the physical origin of disagreements between experiment and simulation. In contrast, the present approach records the creator process, production material, production volume, exit layer, propagation direction, and statistical weight associated with every accepted photon. This infor-mation makes it possible to separate the contributions of proton ionisation, secondary-electron interactions, bremsstrahlung, and proton-induced nuclear reactions without modifying the underlying transport simulation. The event-level audit therefore transforms the simulated spectrum from a simple detec-tor output into a fully traceable physical dataset.

The remaining differences between the simulated and experimental spec-tra are likely to arise from several independent sources. First, the experimen-tal benchmark was reconstructed from a digitized published figure rather than from the original acquisition data. Consequently, small uncertainties associated with graphical digitization, interpolation, and energy calibration inevitably affect the comparison. Secondly, several experimental parame-ters required for an absolute simulation are unavailable in the published documentation. These include the delivered beam charge, acquisition live time, detector dead time, electronic shaping parameters, and the absolute full-energy peak efficiency of the HPGe detector. Because these quantities cannot be reconstructed uniquely, the present work deliberately avoids arbi-trary normalization factors and instead focuses on normalized spectral-shape validation.

Additional discrepancies may originate from uncertainties in the simpli-fied detector-response model adopted during post-processing. Although the applied Gaussian broadening, escape peaks, and low-energy tailing repro-duce the principal characteristics of a planar HPGe detector, the model does not explicitly simulate electronic pulse formation, charge trapping, ballistic deficit, or amplifier response. Likewise, the intrinsic efficiency is represented by a compact attenuation model rather than by a detector-specific calibra-tion curve. These simplifications primarily influence peak widths and abso-lute peak areas but have comparatively little effect on the overall spectral shape considered in the present validation.

The choice of the Livermore low-energy electromagnetic package com-bined with the FTFP_BERT reference physics list proved appropriate for the energy range investigated in this work. The Livermore models provide a detailed description of low-energy photon interactions together with atomic relaxation processes that are essential for realistic PIXE simulation, whereas the hadronic component accurately describes the transport of energetic pro-tons through the multilayer target [6, 8, 12]. Although alternative physics configurations are available within Geant4, the present results indicate that the selected configuration provides a consistent description of both charac-teristic X-ray production and secondary radiation under the published AR-RONAX irradiation conditions.

Compared with previous Geant4 PIXE studies [10, 11], the present work extends the validation in two important respects. First, the simulation is evaluated against a published HE–PIXE benchmark performed at the AR-RONAX facility using a 68 MeV proton beam and a multilayer Cu/Bi target. Secondly, the event-level photon audit provides direct access to the physi-cal origin of every detected photon, allowing the relative importance of the different production mechanisms to be quantified independently. This level of diagnostic information is not available from conventional spectrum scor-ing alone and represents an additional tool for detector optimization and benchmark validation.

The methodology developed here is not restricted to the ARRONAX benchmark. Because the photon-audit framework is implemented at the sim-ulation level, it can be applied directly to other multilayer targets, detector geometries, proton energies, or ion species without modification of the under-lying analysis strategy. The same approach could therefore be employed for future studies involving Ti, Fe, Ni, Ag, Au, or other technologically impor-tant multilayer systems, as well as for detector optimization and uncertainty propagation studies.

Overall, the present investigation demonstrates that the combination of detailed Geant4 transport, transparent detector-response modelling, and event-level photon auditing provides a reproducible framework for interpret-ing HE–PIXE spectra. Although additional experimental information would be required for absolute detector calibration, the normalized spectral com-parison performed here successfully validates the principal physical processes responsible for characteristic X-ray production and establishes a solid basis for future developments in high-energy PIXE simulation.

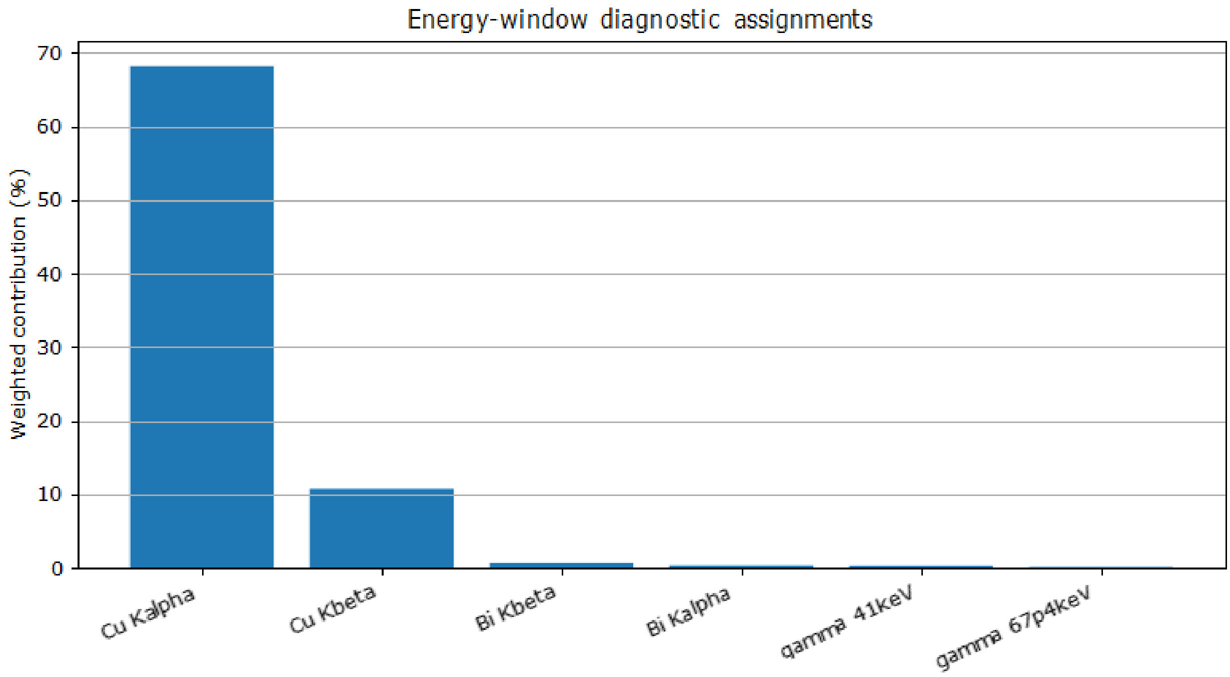

Figure 12: Distribution of photon exit layers for all accepted photons.

8.Conclusions

A physics-audited Geant4 model has been developed for the simulation of the published ARRONAX High-Energy Particle-Induced X-ray Emission (HE–PIXE) benchmark using a 68 MeV proton beam incident on a Cu/Bi multilayer target. The simulation combines detailed particle transport with a transparent detector-response model incorporating air attenuation, trans-mission through the beryllium entrance window, intrinsic HPGe efficiency, Gaussian energy broadening, escape peaks, and low-energy tailing. The pro-cessed simulation was compared with the digitized experimental spectrum over the energy interval from 5–90 keV, enabling a quantitative assessment of the normalized spectral shape.

The comparison demonstrates that the proposed model successfully repro-duces the principal experimental characteristics of the published HE–PIXE spectrum. The dominant Cu characteristic X-ray peaks are correctly repro-duced after detector-response modelling, while the overall continuum exhibits good qualitative agreement with the experimental benchmark. Statistical indicators, including the RMSE, MAE, Pearson correlation coefficient, and coefficient of determination, provide an objective measure of the agreement between the processed simulation and the digitized reference spectrum. Al-though the validation is limited to normalized spectral shapes because the original beam charge, detector live time, and absolute detector calibration were not available, the results confirm that the principal physical processes governing characteristic X-ray production are consistently described by the simulation.

The principal methodological contribution of the present work is the im-plementation of an event-level photon-audit framework. Unlike conventional detector scoring approaches that record only the final detected spectrum, the proposed methodology preserves the complete physical provenance of every accepted photon, including its creator process, production material, produc-tion volume, exit layer, propagation direction, statistical weight, and detected energy. This additional information provides direct insight into the origin of the measured spectrum and enables individual production mechanisms to be investigated independently. The photon-audit methodology therefore constitutes a valuable diagnostic tool for detector optimization, physics-list assessment, uncertainty analysis, and future benchmark validation.

The analysis further confirms that proton-induced atomic ionisation is the dominant mechanism responsible for characteristic X-ray production under the ARRONAX irradiation conditions, whereas bremsstrahlung and proton-induced nuclear reactions contribute primarily to the continuum background. The decomposition of the detected spectrum into its individual physical com-ponents illustrates the capability of the event-level audit to provide informa-tion that is inaccessible through conventional spectrum comparison alone.

Several limitations of the present investigation should nevertheless be recognized. The published benchmark does not provide the experimental beam charge, acquisition live time, detector dead time, channel-by-chan-nel statistical uncertainties, or an absolute detector efficiency calibration. Consequently, the present work deliberately avoids arbitrary normalization procedures and restricts the validation to normalized spectral shapes.

Fur-thermore, the detector-response model is based on a compact analytical de-scription rather than a complete simulation of detector electronics and signal formation.
Future developments will focus on extending the present methodology in several directions. First, experimentally calibrated detector-response func-tions will be incorporated to enable absolute-yield validation. Secondly, the event-level photon-audit framework will be applied to additional multilayer targets and different proton energies in order to investigate the generality of the proposed methodology. Finally, the audit information generated by the simulation will be integrated with machine-learning techniques for automated spectrum interpretation, multilayer characterization, detector optimization, and uncertainty quantification. These developments will further strengthen the role of Geant4 as a transparent and reproducible simulation framework for high-energy PIXE research.

Data and code availability

The accompanying archive contains the complete LaTeX source, archived analysis metrics, comparison data, audit summaries, plotting inputs, and the Geant4 source snapshot used to document the reported configuration. Absolute-yield validation would additionally require experimental beam charge, acquisition live time, and a calibrated full-energy peak efficiency.

Declaration of competing interest

The authors declare that they have no known competing financial inter-ests or personal relationships that could have appeared to influence the work reported in this paper.

References

1. T. B. Johansson, R. Akselsson, S. A. E. Johansson, X-ray analysis: Elemental trace analysis at the 10−12 g level, Nuclear Instruments and Methods 84 (1970) 141–143. doi:10.1016/0029-554X(70)90751-2.
2. S. A. E. Johansson, J. L. Campbell, K. G. Malmqvist, Particle-Induced X-Ray Emission Spectrometry, John Wiley & Sons, 1995.
3. D. D. Cohen, et al., K, l, and m shell datasets for pixe spectrum fitting and analysis, Nuclear Instruments and Methods in Physics Research Section B 363 (2015) 7–18. doi:10.1016/j.nimb.2015.08.021.
4. C. Koumeir, F. Haddad, V. Métivier, N. Servagent, N. Michel, A new facility for high-energy pixe at the arronax facility, in: AIP Conference Proceedings, Vol. 1412, 2011, pp. 105–112. doi:10.1063/1.3665301.
5. D. El Hajjar Ragheb, Développement de la méthode pixe à haute énergie auprès du cyclotron arronax, Ph.D. thesis, École Nationale Supérieure des Mines de Nantes, nNT: 2014EMNA0137; HAL: tel-01062444 (2014).
6. S. Agostinelli, et al., Geant4—a simulation toolkit, Nuclear Instruments and Methods in Physics Research Section A 506 (2003) 250–303. doi: 10.1016/S0168-9002(03)01368-8.
7. J. Allison, et al., Geant4 developments and applications, IEEE Transac-tions on Nuclear Science 53 (2006) 270–278. doi:10.1109/TNS.2006.
8. 869826.
9. J. Allison, et al., Recent developments in geant4, Nuclear Instruments and Methods in Physics Research Section A 835 (2016) 186–225. doi: 10.1016/j.nima.2016.06.125.
10. J. Apostolakis, et al., Geometry and physics of the geant4 toolkit for high and medium energy applications, Radiation Physics and Chemistry 78 (2009) 859–873. doi:10.1016/j.radphyschem.2009.04.026.
11. M. G. Pia, et al., New models for pixe simulation with geant4, IEEE Transactions on Nuclear Science 56 (2009) 3614–3649. doi:10.1109/ TNS.2009.2033506.
12. A. Mantero, et al., Pixe simulation in geant4, X-Ray Spectrometry 40 (2011) 135–140. doi:10.1002/xrs.1314.
13. V. N. Ivanchenko, et al., Recent improvements in geant4 electromag-netic physics models and interfaces, Progress in Nuclear Science and Technology 2 (2011) 898–903. doi:10.15669/pnst.2.898.
14. Geant4 Collaboration, Geant4 physics reference manual, release 11 Se-ries (2024).